# Fluid Dynamics Aided Design of an Innovative Micro-Gripper

Gianmauro Fontana, Serena Ruggeri, Antonio Ghidoni, Alessandro Morelli, Giovanni Legnani, Adriano Maria Lezzi, Irene Fassi

# Fluid Dynamics Aided Design of an Innovative Micro-gripper

Gianmauro Fontana[1[0000-0003-4538-7985]], Serena Ruggeri[1[0000-0002-4303-3297]], Antonio Ghidoni[2[0000-0001-5513-4784]], Alessandro Morelli[2], Giovanni Legnani[2[0000-0002-2700-5093]], Adriano Maria Lezzi[2[0000-0001-5655-0202]], and Irene Fassi[1[0000-0002-6144-2123]]

[1] Institute of Intelligent Industrial Technologies and Systems for Advanced Manufacturing - National Research Council of Italy, Via A. Corti 12, 20133 Milan, Italy
gianmauro.fontana@stiima.cnr.it
[2] Dept. of Mechanical and Industrial Engineering - University of Brescia, Via Branze 38, 25123 Brescia, Italy

**Abstract.** The increasing miniaturization of more and more systems and products is supporting the necessity to develop and handle micro-objects and micro-assembling tools. However, in comparison to bigger scale systems, micro-scale tasks undergo greater challenges due to the effect of unwanted sticking forces whose relative value may be predominant at the micro-scale. Systems to overcome these limiting factors have to be specifically developed to enable an effective and successful manipulation. In the case of contact micro-grippers, specific additional devices or manipulating strategies are used to assure the success of the release phase. In this context, this paper presents an innovative vacuum micro-gripper with a low-cost and simple automatic releasing device which can effectively overcome the adhesive forces. The paper, after illustrating the working principle of the gripper, discusses the preliminary results of a first computational fluid dynamics model useful to represent the main gripper characteristics and able to support a design procedure.

**Keywords:** Vacuum Micro-gripper, Fluid Dynamic Simulations, Micro-gripper Design.

## 1 Introduction

The necessity to manufacture a great variety of different micro-components with different characteristics (material, size, shape, etc.) is the result of the current trend towards the miniaturization of many objects and systems. These small components have to be manipulated and assembled undergoing a set of specifications related to their intrinsic properties including the maximum acceptable stress, the dimension of the area available for gripping, the presence of reference points, or the requirement for specific working conditions. Further constraints may be related to the assembly precision, the necessity to assure the stability of the coupling or to guarantee the possibility of disassembly, the presence of obstacles or the interference with other components. Generally speaking, these requirements appear similar to those for components and

systems with a bigger size, however some physical characteristics make the manipulation at the micro-scale more challenging mainly for the relative importance of the surface forces. In this environment, the adhesion forces between the gripper and the component to be manipulated may greatly influence the task execution. These forces include the van der Waals effect, the electrostatic one, capillary forces and others [1]. Such forces may be stronger than the weight of the component to be manipulated generating a sticking effect, preventing the detachment from the micro-gripper when the release is required and generally making the manipulation more difficult. To overcome these difficulties specific solutions and devices have to be designed to assure an effective manipulation and assembly.

Several different micro-grippers based on contact or contact-less principles have been presented in literature [2-4]. They take advantage of different technologies and strategies like: ultrasonic waves, acoustic, electrostatics, vacuum, capillarity, etc. Considering the contact grippers, a great role is played by vacuum actuators which are used in several industrial applications (for instance in MEMS, mechanical micro-objects, for rework and assembly of electronic boards, etc.). However, vacuum grippers are also used to manipulate biological samples (pick and place) for sample analysis or micro-injection of specific molecules. Vacuum micro-grippers generally have a simple structure, simple actuation, and working principle. They have a wide range of applicability also in the manipulation of fragile components. However, as with all the contact grippers, the adhesive forces may negatively affect their performance preventing their use in some applications.

Different release solutions based on active and passive principles have been described in literature to overcome this difficulty, but the realization of a general, precise, and reliable solution is still an open research field. Generally, active release strategies make use of a supplementary component to provide some actions forcing the detaching of the object from the gripper; other strategies are based on the reduction of the contact area. Other strategies are based on mechanical vibration [5], the generation of positive pressure impulses, the use of a supplementary tool or an edge touching the object to detach [6], snap-fasteners [7], gluing [8] or rolling [9] the object to the release workplace.

Having these issues in mind, this paper proposes an innovative vacuum micro-gripper with the capability to overcome the adhesive forces in a simple and effective way, without the use of additional actuators and preserving the simplicity and light design. This paper also presents a preliminary numerical model based on computational fluid dynamics analysis.

In the next sections, the working principle of this innovative micro-gripper is presented, also considering the evolution from a simpler and more traditional design to an advanced one. Then, the development of a preliminary computational fluid dynamic model is considered to rationally explain the main gripper characteristics and to sketch a rational design procedure.

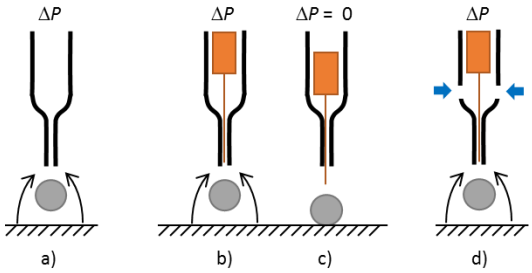


**Fig. 1.** Working principles of some vacuum micro-grippers: (a) traditional, (b, c) first extended design incorporating an automatic releasing system, and (d) final advanced version.

## 2 The working principle of the vacuum micro-grippers

The micro-gripper proposed in this paper is the last prototype of successive evolutions originated from a traditional design (Fig. 1). The prototype marked by a) is a classical vacuum micro-gripper characterized by a very simple but cost effective design that however may suffer from the mentioned sticking problems. A first evolution is shown in Fig. 1 (b, c) which exhibits the presence of a passive automatic releasing device. A "releasing mass" that may move up and down is incorporated inside the body. A pin is embedded in the mass and inserted in the cannula. The mass (and so the pin) is sucked up when the gripper is activated by a negative pressure $\Delta P$. When the gripper is deactivated, the mass falls down and the pin generates a releasing action on the grasped object. More details on this patent design are contained in [10]. The limit of this design is that the limited air flow does not permit the lift of a "big" releasing mass, limiting the detaching capability.

To increase the lifting capabilities some lateral holes have been added to the gripper body (two holes in the case of Fig. 1 (d)). In this case, when the gripper is activated by the negative pressure, a larger air flow is generated and a larger lifting action is obtained. This allows including a bigger releasing mass able to generate a more significant detaching action, also suitable for overcoming high sticking forces. More details are described in [10, 11].

The basic equation for the gripper design (Fig. 1) is

$$F = \Delta P\, A_0 \geq m\, g \qquad A_0 = \frac{\pi d_{ic}^2}{4} \tag{1}$$

which shows the dependence of the grasping force to the cross section area $A_0$ of the cannula and the negative pressure drop $\Delta P$. This permitted forecasting the maximum mass $m$ of the object that can be grasped; $g$=9.81 m/s$^2$ is the gravity acceleration and $d_{ic}$ is the internal diameter of the cannula. If the version with the releasing mass $M$ is considered (Fig. 1 (b, c)), Eq.(1) has to be modified adding $M$ to $m$. An improved model may take into account the presence of a limited airflow between the cannula and the object even when an object has been grasped, because experience shows that

the object never completely seals the cannula [10]. However, this flow is very little and difficult to model.

In the case of the prototype of Fig. 1 (b, c), to overcome the sticking force $F_s$, the mass $M$ of the releasing object has to satisfy the following inequality

$$M\,g \geq F_s - mg$$

Moreover, for the gripper of Fig. 1 (d), it has to be considered that the grasping force is the result of the difference between the pressure $P_1$ of the lower chamber and the outside pressure that in a standard situation is $P_0$=100 kPa (see Fig. 2 (a))

$$F = (P_0 - P_1)\,A_0 \geq m\,g \tag{2}$$

Of course, the pressure $P_1$ depends on the applied negative pressure, and on the geometry of the whole system including the entity of the airflow through the lateral holes.

Preliminary experimental tests have been performed on three different prototypes whose main characteristics are shown in Table 1 and Fig. 2 (b). The tests conditions considered different pressure values and different lateral holes areas obtained by partially occluding them, then simulating different equivalent diameters. The variation of the cross section of the lateral hole proved to be an important factor greatly affecting the gripper performance: if the hole is too small, the air flow decreases significantly and the lifting force becomes insufficient to lift the releasing mass. Oppositely, a larger hole generates a too large airflow with a consistent reduction of the pressure drop $\Delta P = P_0 - P_1$ in the lower chamber, degenerating the grasping performance of the gripper. It was concluded that an optimal value of the diameter of the later holes exists and had to be identified. In order to formulate a numerical procedure to design the micro-gripper and to identify its main characteristics, a fluid dynamic model was developed and is illustrated in the following Sections.

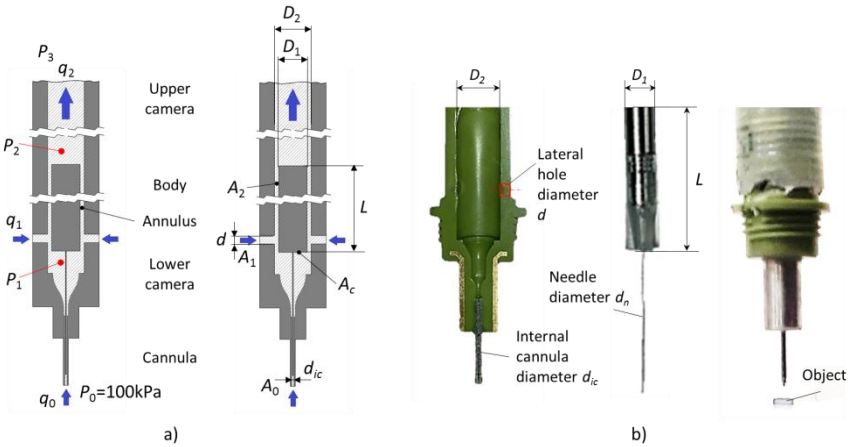


**Fig. 2**. Vacuum micro-gripper with additional air flows: a) the model and the parameters used in the simulations; b) a prototype.

**Table 1.** Main characteristics and dimensions of the micro-gripper of Fig. 2 (b).

| Identification Code | Needle diameter $d_n$ [μm] | Inner cannula diameter $d_{ic}$ [μm] | Body diameter $D_2$ [mm] | Mass diameter $D_1$ [mm] | Mass length $L$ [mm] | Mass $M$ [mg] | Lateral hole diameter $d$ [μm] |
|---|---|---|---|---|---|---|---|
| 0.2 | 79 | 139 | 3.6 | 2.4 | 24.2 | 707 | 766 |
| 0.25 | 79 | 152 | 3.6 | 2.4 | 24.2 | 707 | 766 |
| 0.3 | 145 | 208 | 3.6 | 2.4 | 24.2 | 707 | 766 |

## 3 CFD simulations

The gripper has been analyzed through a Computational Fluid Dynamics (CFD) tool, the open source CFD toolbox OpenFOAM® [12, 13], to compute the air velocity, pressure, and temperature fields inside the device. The post-processing of the computed results provides also the air mass flow rate through the cannula and the lateral holes, and the forces applied by the air on the gripper inner surfaces, such as the lifting forces on the releasing mass [14]. The aim of these simulations is to support the design of new optimized prototypes, investigating the effect of gripper geometry modifications on its performance.

The compressible steady-state solver *rhoSimpleFoam* has been used to solve the RANS (Reynolds Averaged Navier-Stokes) equations coupled with the SST turbulence model (low Reynolds number version, i.e. without wall functions). All the simulations were run in parallel on a Linux workstation (Intel Core i7 970, six cores at 3.2 GHz).

For the simulations, a simplified gripper geometry has been considered, as shown in Fig. 2 (a). Table 2 reports the values of the geometric parameters ($L$, $d$, $D_1$, and $D_2$) adopted in the simulations. Nominal values correspond to the original configuration. Modified configurations were obtained varying the parameters $L$, $d$, and $D_2$, one at a time (see Table 2). 7 configurations were tested, considering three different outlet pressures $P_3$ (70, 80, 90 kPa) at the outlet section: 21 CFD simulations were performed.

**Table 2.** Geometric parameters and related values for the CFD simulations. Dimensions in [mm].

| Parameter | Minimum | Nominal | Maximum |
|---|---|---|---|
| $L$ | 16.2 | 24.2 | 32.2 |
| $d$ | 0.5 | 0.77 | 1 |
| $D_1$ | | 2.6 | |
| $D_2$ | 3.2 | 3.4 | 3.6 |

The “optimal” mesh density for the simulations has been determined through a grid independence analysis. The air mass flow rate and the lifting force have been monitored on a coarse ($222\times10^3$ cells), a medium ($473\times10^3$ cells), and a fine ($767\times10^3$

cells) grid, made of hexahedral and tetrahedral elements. The choice not to use wall-functions requires the size of the elements adjacent to the solid walls to be fine enough to compute the boundary layer accurately (i.e., non-dimensional thickness of the elements, $y^+$, was set equal to 1 for all meshes).

The medium grid has been used for all the simulations, showing best results in term of accuracy (the relative difference with respect to the results computed on the fine grid is less than 1% for the mass flow rate, and less than 2% for the lift), and saving in computing time. All the simulations lasted about 1.5 hours.

The predicted air mass flow rate through the lateral holes ranges between $4.8 \times 10^{-5}$ and $28.9 \times 10^{-5}$ kg/s, and the lifting force between 3.6 and 81 mN. This force is the sum of two contributions: (i) the form component, depending on the pressure difference $P_1$-$P_2$, (about 85% of the total force as shown by the simulations); (ii) the skin friction component, due to the viscous stresses acting on the lateral surface of the releasing mass (about 15% of the total force).

The flow field inside the gripper is characterized by low velocities. Only the inlet zone of the cannula and of the lateral holes (see Fig. 3) are characterized by a Mach number Ma = $v/c \cong 0.5$ (with $v$ the air velocity, and $c$ the corresponding speed of sound), nevertheless the presence of these two zones of high velocities forced the use of a compressible solver.

Fig. 4 shows the pressure contours, characterized by a fast decrease of the static pressure at the inlet zone of the cannula and of the lateral holes, and a linear decrease along the meatus from the lateral holes to the end of the releasing mass.

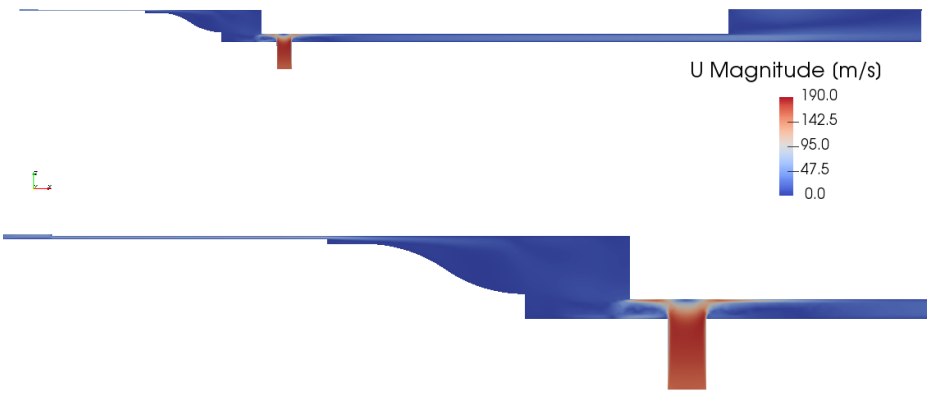


**Fig. 3.** Velocity field for the nominal case of Table 2, $P_3$=80 kPa.

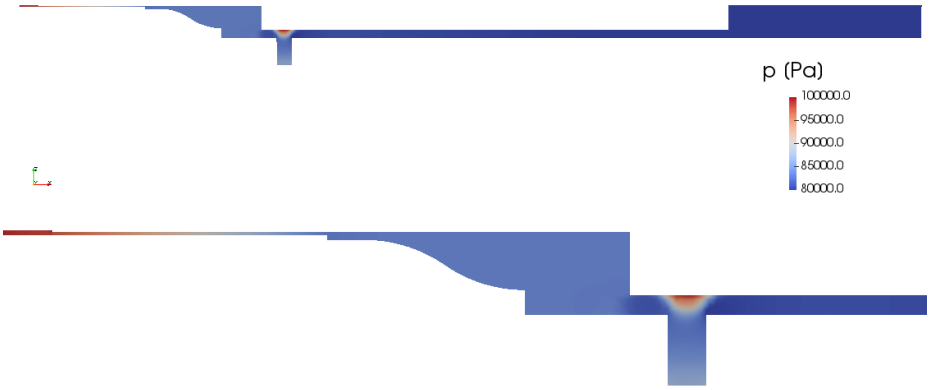


**Fig. 4.** Pressure field for the nominal case of Table 2, $P_3$=80 kPa.

It was also verified that the pressure drop $\Delta P_1=P_0-P_1$, between the outside and the lower chamber, is much greater than the pressure drop $\Delta P_3=P_1-P_3$, between the lower and the upper chamber. Moreover, the zone with the lowest pressure $P_2$ is located in the upper chamber, just behind the releasing mass. So

$$P_0-P_1 >> P_1-P_2 > P_1-P_3 \qquad P_0 > P_1 > P_3 > P_2$$

This behavior is due to the fact that the cannula cross section area is much smaller than the lateral holes area and the annulus area

$$A_0 << A_1 < A_2$$

## 4 The gripper model

In order to establish a set of approximate correlations to describe the fluid dynamics of the gripper, it may be useful to refer to the following parts of the device: cannula, lower chamber, lateral holes, annulus (between the releasing mass and the body), upper chamber.

There are three air mass flow rates of interest: the one through the cannula and the lower chamber, $q_0$; the one through the lateral holes, $q_1$; and the one through the annulus and the upper chamber, $q_2$, which is the sum of the other two:

$$q_2 = q_1 + q_0 \tag{3}$$

Since the cannula area is about 2% of the lateral holes area, a flow rate $q_0$ much smaller than the flow rate $q_1$ was expected. Simulations performed to compare results with and without flow through the cannula (closed cannula, $q_0$ = 0) prove that the flow rate $q_0$ does not affect for all practical purposes either the pressure field in the

gripper or the force acting on the releasing mass: for this reason, in what follows it will be neglected

$$q_2 \cong q_1 \tag{4}$$

The flow rate $q_1$ and the pressure difference between the atmospheric pressure $P_0$ and that of the lower chamber $P_1$ are strongly coupled. On the basis of theory and experience, the following empirical expression was assumed:

$$P_0 - P_1 = k_a \frac{q_1^{n_a}}{d^{m_a}} \tag{5}$$

where $d$ is the diameter of the holes, and $n_a$, $m_a$ and $k_a$ are suitable constants. The values of the constants were estimated using the least squares method to fit the computational results: these values are reported in Table 3. The pressure drop can be predicted with an average error of 3% and a maximum error of 7% (see Fig. 5 (a)).

The pressure drop between the lower and the upper chambers is coupled to the air flow through the device. The main geometrical parameters that influence this pressure drop are the annulus area $A_2$ and length $L$. The following empirical expression was assumed to take into account a factor proportional to the annulus length $L$ and a factor depending on the abrupt enlargement from the annulus into the upper chamber

$$P_0 - P_3 = k_1 \frac{q_2^{n_1}}{A_1^{m_1}} + k_2 \frac{q_2^{n_2}}{A_2^{m_2}} + k_3 L \frac{q_2^{n_3}}{A_2^{m_3}} \quad \text{with} \quad A_1 = \frac{\pi}{4} d^2 \;;\; A_2 = \frac{\pi}{4}\left(D_2^2 - D_1^2\right) \tag{6}$$

The values of constants $k_i$, $m_i$ and $n_i$ were estimated to fit the results of the simulations (Table 3). These coefficients allowed predicting the pressure drop $\Delta P = P_0 - P_3$ with an average relative error of 2.2% and a maximum error of 5%.

In a similar way, an empirical model was built to predict the lifting force $F_{tot}$ which is the sum of two contributions. The first one, $F_p$, is proportional to the pressure difference $P_1$-$P_2$ and to the cross sectional area $A_c$ of the releasing mass. The second contribution, $F_v$, is due to the viscous stress exerted on the lateral surface $A_l$ of the releasing mass by the air flow. The following empirical model was assumed

$$F_p = k' \frac{\pi}{4} D_1^2 \left(P_1 - P_2\right) \cong k_4 \frac{v^{n_4}}{\left(D_2 - D_1\right)^{m_4}} \qquad F_v = k'' A_l \mu \frac{\partial v}{\partial r} = k_5 L \frac{v^{n_5}}{\left(D_2 - D_1\right)^{m_5}}$$

$$F_{tot} = F_p + F_v \qquad F_v \cong 0.15 \times F_{tot} \tag{7}$$

where $v$ is the average velocity in the annulus $v = q_2/\rho A_2$, $\rho$ is the density which depends on the pressure $\rho = P/(R^* T)$, $R^*$ is the gas constant, $\mu$ is the air viscosity, $\partial v/\partial r$ is the derivative of the velocity with respect to the radial position evaluated for $r = D_1/2$, and $k_i$ are suitable constants. $D_1$ is constant in the considered simulations and its effects are included in $k_4$. The value of the constants which permit predicting the lifting force with an average error of about 0.9 mN and a maximum error of 3 mN (see Fig. 5 (b)) are reported in Table 4.

**Table 3.** Constants of the empirical model to predict the pressure drops as a function of the geometry and of the air mass flow rate (Eq.s (5) and (6)). Dimensions in [mm], flow rate in [kg/s], pressures in [kPa].

| Subscript $i$ | $k_i$ | $n_i$ | $m_i$ |
|---|---|---|---|
| $a$ | $2.425\ 10^{9}$ | 2.295 | 5 |
| 1 | $6.63\ 10^{9}$ | 2.284 | 2.5 |
| 2 | $1.07\ 10^{9}$ | 1.898 | 2.5 |
| 3 | $1.19\ 10^{7}$ | 1.792 | 2.5 |

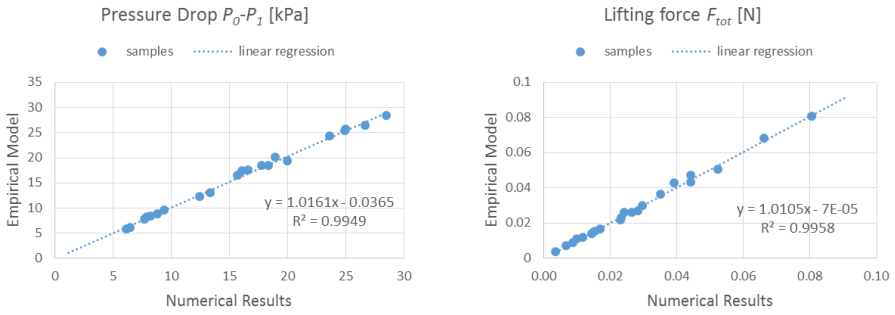


a) b)

**Fig. 5.** Comparison of the CFD simulations with the result of the empirical model for the prediction of: (a) the pressure drop $P_0$-$P_1$; (b) the lifting force. Data points, regression equation, and linear regression coefficient $R$.

**Table 4.** Constants of the empirical model to predict the lifting force as a function of the geometry and of the air flow rate (Eq. (7)). Forces in [N].

| | Subscript $i$ | $k_i$ | $n_i$ | $m_i$ |
|---|---|---|---|---|
| $F_p$ | 4 | $3.54\ 10^{-5}$ | 1.547 | 0.8180 |
| $F_v$ | 5 | $1.83\ 10^{-6}$ | 1.454 | 0.2885 |

## 5 The design procedure

The model presented was not precise enough to be directly adopted for an optimized gripper design, however it can be used to start a recursive trial and error procedure based on finite elements fluid dynamics simulations. The model can help in choosing the parameters and reducing the required simulations. The design procedure may be composed of the following steps:

1. The object to be grasped is examined to estimate its mass $m$ and the sticking force $F_s$ to be overcome. Theoretical or experimental tests have to be performed for each specific situation.
2. The diameter $A_0$ of the cannula is chosen in function of the geometrical size of the object to be grasped. The experience suggests the rule of thumb according with the diameter of the cannula should be at least 20% of the equivalent diameter of the part [15]. The pressure value in the lower chamber is then chosen by applying Eq. (2):

$$P_0 - P_1 \geq \lambda \frac{mg}{A_0} \tag{8}$$

   where $\lambda \geq 1$ is a safety factor to take into account the actual operating dynamic conditions, for instance high acceleration of the gripper when carrying an object.
3. The mass $M$ of the releasing device is then chosen in order to generate a sufficient force to overcome the sticking force $F_s$:

$$M \geq \frac{F_s}{g} - m \tag{9}$$

   and knowing the mass a first value for its dimensions is established.

4. The lifting force $F_r > Mg$ is then chosen and consequently the size of the releasing mass, and the value of the pressure $P_2$ is hypothesized according to Eq. (7) and considering

$$F_{TOT} \cong 1.2 F_p$$

5. The air flow $q_2$ and the last geometrical dimensions are chosen according to Eq. (6).

The results can be adjusted performing few iterative adjustments. The proposed procedure permitted finding an approximate value for the main parameters of the gripper that can be used to generate a model to be analyzed by some finite element fluid dynamic model. This model can be iteratively modified to perform the final design.

## 6 Conclusions

The paper presents an innovative micro-gripper incorporating an automatic releasing system and its design procedure.

A prototype of this type of micro-gripper was developed and proved to reliably overcome the adhesive forces when grasping and releasing objects.

A numerical model, based on preliminary finite element fluid dynamics analysis, showed how the gripper geometry affects its performance, and was then exploited for a first design of the gripper. Indeed, Computational Fluid Dynamic- (CFD) simula-

tions are used to identify the unknown model parameters by the least squares method in order to predict the air mass flow rates and the forces applied on the surfaces, such as the lifting forces on the releasing mass. However, at the moment, the model is not sufficiently precise to replace a detailed CFD analysis, but it is able to highlight the main characteristics of the gripper. The model will be improved considering more simulations to include combined effects of the parameters and results of experimental tests. The present results, however, confirm the first experimental results reported in [11].

Each CFD simulation is very time consuming (it requires a couple of hours of computation in addition to the time required to create the mesh and adjust all the parameters), whilst the empirical model can be solved in less than one second and the form of the equations suggests the influence of each parameter. Although for a full detailed design procedure the model has to be validated with experimental tests, at this stage it is able to explain the behavior of the gripper and to suggest indicative values for its practical design.

Finally, the gripper design procedure, based on this empirical model, is explained step by step, in order to choose the gripper geometry and the working parameters compliant with the manipulation specifications, such as the object mass and the sticking forces.

## Acknowledgments

The work has been partially supported by the project: “Cybersort” - 3AQ CNR Regione Lombardia. The authors thank Fabio Colombo for his contribution, during his Master’s thesis development, to the investigation on the presented micro-gripper.

## References

1. Fearing, R.S.: Survey of Sticking Effects for Micro Parts Handling. In: Proc. of IEEE/RSJ Int. Conf. on Intelligent Robots and Systems, Human Robot Interaction and Cooperative Robots, vol. 2, pp. 236-241, IEEE (1995).
2. Gauthier, M., Lambert, P., Régnier, S.: Microhandling and Micromanipulation Strategies. In: Chaillet, N., Régnier, S. (eds.) Microrobotics for Micromanipulation, Chap. 3, pp. 179-242. Wiley-ISTE, Great Britain (2010).
3. Fantoni, G., Porta, M.: A critical review of releasing strategies in microparts handling. In: Ratchev, S., Koelemeijer, S. (eds.) Micro-Assembly Technologies and Applications. IPAS 2008. IFIP — International Federation for Information Processing, vol. 260, pp. 223-234, Springer, Boston, MA (2008).
4. Khan, S., Sabanovic, A.: Force feedback pushing scheme for micromanipulation applications. Journal of Micro-Nano Mechatronics 5(43), 43-55 (2009).
5. Haliyo, D. S., Régnier, S., Guinot, J. C.: µMAD, the adhesion based dynamic micromanipulator. European Journal of Mechanics - A/Solids 22(6), 903-916 (2003).
6. Zesch, W., Brunner, M., Weber, A.: Vacuum tool for handling microobjects with a Nano-Robot. In: Proc. of the 1997 IEEE ICRA, vol. 2, pp. 1761-1766, IEEE (1997).

7. Prasad, R., Böhringer, K. F., MacDonald, N. C.: Design, Fabrication, and Characterization of Single Crystal Silicon Latching Snap Fasteners for Micro Assembly. In: Proc. of ASME IMECE'95, 57(2), pp. 917-923 (1995).
8. Bark, C., Binnenböse, T., Vögele, G., Weisener, T., Widmann, M.: Gripping with low viscosity fluids. In: Proc. of the IEEE Eleventh Annual International Workshop on Micro Electro Mechanical Systems (MEMS'98), IEEE, pp. 301-305 (1998).
9. Haliyo, D. S., Dionnet, F., Regniér, S.: Controlled rolling of microobjects for autonomous manipulation. Journal of Micromechatronics, 3(2), 75-101 (2006).
10. Ruggeri, S. Fontana, G. Legnani, G., Fassi, I.: Design strategies for vacuum micro-grippers with integrated release system. In: Proc. ASME IDETC, vol. 4, pp. V004T09A022 (2017).
11. Colombo, F.: Modelization and optimization of a vacuum gripping-releasing device for micromanipulation. Master Thesis in Industrial Automation Engineering, University of Brescia, Brescia, Italy (2016).
12. Weller, H. G., Tabor, G., Jasak, H., Fureby, C.: A tensorial approach to computational continuum mechanics using object-oriented techniques, Computers in Physics, 12 (6), (1998).
13. OpenFOAM 4.1 Webpage, https://openfoam.org, last accessed 2017/12/06.
14. Morelli, A.: Modellazione e simulazione numerica di deflussi in microdispositivi di presa ad aspirazione (*Modeling and numerical simulation of flows in suction gripping microdevices)*, Master Thesis in Mechanical Engineering, University of Brescia, Brescia, Italy (2017).
15. Fontana, G., Ruggeri, S., Fassi, I., Legnani, G.: A mini work-cell for handling and assembling microcomponents. Assembly Automation 34(1), 27-33 (2014).